Biochimica et Biophysica Acta, 1153 (1993) 111–121

BBAMEM 76125

Functional and biochemical characterization of the human potassium channel Kv1.5 with a transplanted carboxyl-terminal epitope in stable mammalian cell lines

Louis H. Philipson, Andrew Malayev, Andrey Kuznetsov, Christine Chang and Deborah J. Nelson

The University of Chicago, Departments of Medicine, Neurology and the Committee on Cell Biology, Chicago, IL (USA)

(Received 17 March 1993)

Key words: Delayed rectifier; Potassium ion current; Potassium ion channel; Epitope; Characterization; (Human)

The role of the C-terminal domain of the hPCN1/Kv1.5 delayed rectifier K^+ channel was investigated in transfected stable cell lines employing antipeptide and anti-epitope antibodies against hPCN1-cp, an epitope-fusion gene carrying additional sequences encoding a 32 amino acid C-terminal extension. Both wild-type and chimeric genes showed high levels of K^+ channel expression. Detailed electrophysiologic characterization showed there to be no significant effect of the C-terminal extension on channel activity. Immunoblots of whole-cell and membrane preparations demonstrated primarily intact protein in which the C-terminal extension was not cleaved from the peptide chain. Two bands were visualized from cells transfected with either the wild-type or chimeric channels; the slower migrating band was a non-*N*-glycosylated form. The epitope-fusion method will be a useful adjunct to studying the role of functional domains in ion channels, and may provide a means for rapid affinity purification of channel protein.

Introduction

Multiple gene families of mammalian voltage-dependent K^+ channels have recently been described which show extensive sequence homology to the *Drosophila Shaker* gene products and several related loci (for reviews of mammalian isoforms see Refs. 1 and 2). While the N-terminal cytoplasmic domain has been implicated in fast inactivation of A-type channels [3] and plays a role in subunit assembly [4], the role of the variable C-terminal cytoplasmic domain has been less well studied. Among different K^+ channel gene families this domain varies in length from less than one hundred to about a thousand amino acid residues. In addition to potential protein kinase A and C phosphorylation sites contained in the C-terminal domain, several channels with the same transmembrane organization as the *Shaker* family contain sequences which may be critical for channel regulation in this region. For example, the *Drosophila slo* gene product possesses an EF-hand motif in the terminal cytoplasmic domain [5], and both the *Drosophila eag* gene and cyclic nucleotide-gated channels contain a domain homologous to the cGMP binding region of cGMP-activated kinases in the C-terminal segment [6] suggesting that the C-terminal participates in gating events. The importance of this region in functional expression has been demonstrated by deletional mutagenesis. In the mouse channel Kv2.1, C-terminal deletion resulted in loss of channel expression in *Xenopus* oocytes that was restored by reciprocal deletions in the N-terminal domain [7]. A C-terminal deletion was found to cause dominant-negative suppression of K^+ channel function in transgenic *Drosophila* [8]. Whether the channels with C-terminal deletions are correctly transported to the cell surface is unknown.

In order to further characterize the role of the C-terminal domain in the mammalian non-inactivating K^+ channel Kv1.5, we have constructed a chimera, hPCN1-cp, in which sequences encoding the 32 amino acid c-peptide region of human proinsulin has been transplanted to the 3′ end of the hPCN1/Kv1.5 gene. A high-titer antibody directed against the human c-peptide allowed us to verify the reading frame and sequence at the 3′ end, confirming the sequence compared to a recently reported 3′ variant sequence [9]. The human proinsulin c-peptide epitope in conjunction

Correspondence to: L.H. Philipson, Department of Medicine, MC1027, University of Chicago, 5841 S. Maryland, Chicago, IL 60637, USA. Fax: +1 (312) 7029194.

with an anti-peptide antibody directed at the first extracellular loop allowed the detection of the expressed channel by immunohistochemical techniques. Electrophysiological comparison of stable CHO cell lines expressing native hPCN1/Kv1.5 with lines expressing the hPCN1-cp chimera failed to reveal significant differences in channel kinetics. These experiments showed that there was no significant loss of the C-terminal domain and demonstrated partial glycosylation of the channel in the transfected CHO cells.

Expression of the chimeric channel directed by the CMV promoter in CHO cells provides a convenient system for the biochemical and functional-domain analysis of a mammalian K^+ channel in a mammalian fibroblast environment. We conclude that the epitope-fusion method allows detection of a targeted domain in a functional K^+ channel, making this a useful tool in the biochemical characterization of this channel with immunochemical methods.

Materials and Methods

Construction of the pCMV-hPCN1 expression plasmid

Standard procedures were as described previously [10]. The hPCN1/Kv1.5 cDNA was excised from a *Xenopus* oocyte expression vector pSP64T [11] at the upstream Sph1 site (to remove an ATG not in the reading frame) and the downstream *Eco*RV site, which had been converted to a *Bgl*II site previously and subcloned into the pCMV5 plasmid [12]. Co-transfection of the DG-44 $DHFR^-$ line of CHO cells with the pCMV-hPCN1 and pSV2-neo was performed using a modification of the calcium-phosphate precipitation method (BRL) or electroporation, and positive clones selected by growth in the presence of 400 μg/ml of G418.

Construction of the hPCN1-c-peptide chimera

A three-primer, polymerase chain reaction-based method [13] was employed to generate a fusion gene, as follows: the 5′ primer (GAAACGGATCACGAG, bp1692–1706 of hPCN1) was 5′ to the unique *Afl*II site at nucleotide 1719 of hPCN1; the bridging primer (CAGGTCCTCTGCCTC-ACACAAATCTGTTTC), which included 15 bases identical to the 5′ end of the human proinsulin c-peptide coding region [14], excluding codons for the dibasic ends, and 15 bases identical to the 3′ end of the hPCN1/Kv1.5 coding region, except that the TGA stop codon was altered to TGT, coding for cysteine; the 3′ primer (CTCTTCCTTAAG-GACCA-CTACTGCTAGGGACC) included the last 14 bases of the proinsulin c-peptide 3′ end, altering the initial lysine at the C-A junction to TAG, a new stop codon, and created a new *Afl*II site at the 5′ end of this primer. The PCR [15] was then preformed with the three primers and both pSP64T-hPCN1 and pGEM4Z-phins (human preproinsulin cDNA, gift of S. Chan, University of Chicago), in a single tube essentially as described [13], empirically adjusting the concentration of the bridging primer for maximum yield of the fusion product. Amplified products of the correct size were subcloned into the p1000 plasmid (Invitrogen), and five independent clones sequenced completely in both directions. All sequences were as predicted. The fusion gene-fragment was excised by *Afl*II digestion and then subcloned into the *Afl*II site of pCMV-hPCN1 and pSP64T-hPCN1. The correct orientation was determined by DNA sequencing. These clones were designated pSP64T-hPCN1-cp, and pCMV-hPCN1-cp.

Whole-cell and excised outside-out patch current recording from transfected CHO cells

Whole-cell and outside-out excised patch recordings were made according to the methods of Hamill et al. [16]. In both whole-cell and excised, outside-out configurations the internal (pipette) solution was (in mM): 140 KCl, 2 $MgCl_2$, 2 $CaCl_2$, 11 EGTA-KOH, and 10 Hepes (pH 7.2). The external (bath) solution was (in mM): 140 NaCl; 5.4 KCl; 2 $CaCl_2$; 1 $MgCl_2$; 10 Hepes (pH 7.4). Transfected CHO cells had a mean capacitance of 29 ± 9 pF ($n = 24$). Whole-cell membrane conductance was measured in external solutions containing 150 mM K^+ between -10 and 10 mV in a voltage range where channel open-state probability is high and current amplitude is low, thereby minimizing series resistance artifacts in cells with high levels of K^+ channel expression. Measurements of series resistance under these conditions allowed accurate determination of specific membrane conductance which was calculated to be 9.6 ± 6.0 nS/pF ($n = 3$).

Outward current activation was fitted with a fourth power exponential, of the form

$$I = A + B(1 - \exp[-(t - d)/\tau])^4 \quad (1)$$

where A represents a linear leak current component, B represents the peak current amplitude obtained for a given depolarization, and d the delay in current activation. In order to fit the initial phase of the current trace, it was necessary to impose a delay (d) in the current response of the cell to the applied voltage step. The delay was detectable only for depolarizations greater than 0 mV and was 0.5 ± 0.13 ms ($n = 22$) +50 mV.

The parameters of steady-state inactivation were determined in experiments in which the holding potential was varied between -80 to +10 mV for 30 s prior to the application of test pulse to +20 mV. The conductance versus voltage (I–V) relationship was determined from deactivating tail currents at -40 mV.

Conductance data were fitted with a Boltzmann distribution.

For recovery from inactivation, the normalized difference between the peak and the non-inactivating component of the outward current in response to the test pulse was plotted against the duration of the interpulse interval. The data were fitted to the sum of two rising exponentials:

$$I = 1 - (A \cdot \exp[-t/\tau_1] + B \cdot \exp[-t/\tau_2]) \quad (2)$$

Immunoblot of Xenopus oocyte membranes

After microinjection of *Xenopus* oocytes as previously described [10] with cRNA prepared from pSP64T-hPCN1-cp, oocyte membranes were prepared by gentle homogenization and sucrose density centrifugation. Membranes were solubilized and size fractionated by SDS-PAGE, and proteins transferred to membranes for immunodetection using anti-c-peptide antibody (gift of K.S. Polonsky, University of Chicago).

RNA blot analysis of transfected cell lines

Total RNA from transfected and control cell lines was prepared by guanidinium-isothiocyanate extraction and centrifugation through CsCl [17], size fractionated in 1% agarose-formaldehyde by gel electrophoresis, and transferred to a nylon hybridization membrane (Genescreen Plus, Dupont). hPCN1/Kv1.5 cDNA was labeled with 32P-dCTP with T7 DNA polymerase and oligonucleotide primers (Megaprime, Amersham). The membrane was pre-hybridized and hybridized as described [18] subjected to a final wash in 0.1% standard saline citrate containing 0.1% SDS for 30 min at 60°C, then exposed to Kodak X-omat AR film for 16 h at −80°C.

Immunohistochemical detection of CHO cells expressing hPCN1 and hPCN1-c-peptide

CHO cells were fixed in 3% formaldehyde, permeabilized with 0.1% Triton X-100, and treated consecutively with: rabbit anti-human-c-peptide antisera or anti-h1-(s1 : s2) peptide antisera (see below) at various dilutions; goat biotinylated anti-rabbit IgG; (Biotin-HRP)-avidin complex; and finally DAB substrate.

Immunoblot analysis of native and N-glycanase-digested hPCN1-cp

Cells expressing the hPCN1-cp gene were scraped from dishes, homogenized in isotonic sucrose buffer, large debris removed by low speed centrifugation, and the 100 000 × *g* pellet was solubilized in *N*-glycanase (GenZyme) buffer containing SDS. Aliquots were incubated for 18 h with or without *N*-glycanase, size-fractionated by polyacrylamide gel electrophoresis, and proteins transferred to nylon membranes. Immunodetection of epitope-bearing proteins was done with anti-human c-peptide antisera or anti-h1-(s1 : s2) antisera using a chemiluminescence method (Amersham ECL detection system).

FACS analysis of transfected cell lines

Rabbit antisera prepared against the peptide H1(s1-s2) LLRHPPAPHQ-PPAPAPGANGSGVMA (amino acid 281–305 in the first putative extracellular loop) derivatized with keyhole limpet hemocyanin (Babco, Richmond, CA), was employed to sort transfected cells expressing hPCN1, hPCN1-cp, and transfected but non-expressing controls. Cells were treated in the following order: rabbit anti-H1(s1-s2) antisera; biotinylated goat anti-rabbit IgG; avidin conjugated with phycoerythrin. Sorting was both analytical and preparative. The cells were sorted on a Coulter Epics 753 with an argon laser emitting at 488 nm. In preparative experiments the brightest and dimmest 10–15% were determined, gates set on this population, and cells sorted at a rate of 2000 cells per second.

Results

A PCR-based technique was employed to construct a chimeric gene in which the 3′ end of the hPCN1 coding region was fused with a cDNA fragment encoding the human proinsulin c-peptide. The resulting new sequence, from the last three residues of hPCN1, is shown in Table I. After the end of the transmembrane domain H6 (aa516–613), hPCN1/Kv1.5 has only 97 residues of which the first 15 are highly conserved among other *Shaker* isoforms. The c-peptide adds 32 residues including the first cysteine (added as linker to replace the stop codon (TGA → TGT)), of which five are negatively charged (Glu/Asp).

An autoradiogram of a RNA blot of transfected but non-expressing CHO cells and transfected expressing clones after hybridization with ^{32}P-labeled hPCN1 probe is shown in Fig. 1. The chimeric mRNA migrates slightly behind the wild-type channel message, confirm-

TABLE I

Nucleotide sequence and deduced amino acid sequence of the 3′ end coding region of the hPCN1-c-peptide fusion gene

Sequences from hPCN1/Kv1.5 starting at amino acid 610 are shown in bold type, followed by the first five and then the last four of the 31 human proinsulin c-peptide residues. The indicated cysteine (*) was generated by the mutation of the TGA stop codon to TGT, and the new stop codon (TAG **) was generated by the mutation of the lysine codon AAG at the C-B junction of human preproinsulin.

...Glu Thr Asp Leu Cys * Glu Ala Glu Asp Leu.....
...GAA ACA GAT TTG TGT * GAG GCA GAG GAC CTG.....
...Gly Ser Leu Gln ---
...GGG TCC CTG CAG TAG **....

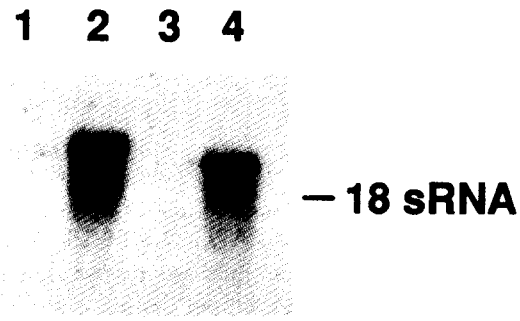

Fig. 1. Autoradiogram of RNA blot analysis of CHO cell lines expressing hPCN1/Kv1.5 and hPCN1-cp. 20 μg of total RNA was applied to each lane and hybridized with hPCN1/Kv1.5 probe as described under Experimental Procedures. Lane 1, mixed culture of 10% positive cells for hPCN1-cp expression; Lane 2, hPCN1-cp expressing cell line; Lane 3, transfected, neo resistant CHO cells negative for K^+ currents; Lane 4, hPCN1/Kv1.5 expressing cell line.

ing its increased size (by 96 nucleotides). The blot was stripped and re-hybridized with labeled preproinsulin cDNA probe and in this case only the fusion-gene mRNA band was visualized (data not shown).

Representative currents recorded from cells transfected with hPCN1/Kv1.5 cDNA are illustrated in Fig. 2. Peak whole-cell current magnitude at depolarizations of +50 mV frequently exceeded 6.0 nA reaching maximal levels of 13–20 nA (Figs. 2A and 2B). The lack of current inactivation over a period of 1 s (Fig. 2A) was probably due to high levels of channel expression resulting in the loss of voltage control in whole-cell experiments. In order to ensure adequate voltage control, further current characterization was carried out using excised outside-out patches. A representative current recording and associated current–voltage (I–V) relationship from a single outside-out patch experiment is shown in Figs. 2C and 2D. Outward current activation was not observed in non-transfected cells or neo-resistant clones that were negative for channel expression in RNA-blots. Current inactivation in outside-out patches was approx. 15–20% complete during a 1-s depolarizing pulse (see Fig. 2C), a time-course similar to that observed in current recordings from oocytes expressing hPCN1/Kv1.5 [10]. The time-course of current inactivation recorded over a period of 30 s was described as the sum of two decaying exponentials with time constants at 0 mV of 1.3 ± 4 and 17.0 ± 5.5 s ($n = 9$), respectively.

Unitary properties of the hPCN1/Kv1.5 K^+ channels in transfected CHO cells are shown in Figs. 2F–2I. Records in which single channel openings were resolvable were rarely seen due to the high levels of channel expression. The time-course of the averaged unitary currents during repetitive depolarizations in patches where single events were resolvable was similar to that observed in the outside-out patches where channel density was high (Fig. 2G). In patches in which single channel events could be resolved, the I–V relationship was linear over the entire outward current range with an average conductance of 12 pS (Fig. 2I). The ionic selectivity of hPCN1/Kv1.5 expressed in mammalian cells was similar to that determined for channel expression in *Xenopus* oocytes [10] and consistent with channels being highly selective for K^+ over Na^+ or Cl^- (Fig. 3).

The threshold for current activation in whole-cell mode was approx. −30 mV while in excised outside-out patches the threshold for current activation was −50 mV. The time-course of outward current activation was well fit with a fourth power exponential. Calculated fits to the activation phase of the outward current records are shown as smooth lines in Fig. 4A. The time constant for current activation decreased with increasing depolarization. At −20 mV the time constant was 8.0 ± 1.9 ms ($n = 22$) decreasing to a value of 0.96 ± 0.19 ms ($n = 22$) at +50 mV.

Steady-state inactivation and conductance-voltage relationships for hPCN1 K^+ currents are given in Fig. 4B. Steady-state inactivation became apparent at holding potentials positive to −60 mV. Complete current inactivation was achieved at potentials positive to −10 mV. The average midpoint of steady-state inactivation as determined from Boltzmann fits to the current data

Fig. 2. Representative whole-cell and excised outside-out patch current records from CHO cells transfected with hPCN1. (A) Family of outward whole-cell K^+ currents in response to voltage steps from a holding potential of −70 mV to test potentials between −100 and +50 mV in 10 mV increments. Step potential changes were applied at 15 s intervals. The data were low pass filtered at 500 Hz and sampled at 1 kHz. (B) Peak current amplitude plotted as a function of membrane potential. (C) Currents recorded from an outside-out patch obtained from the same cell. (D) Peak current amplitude plotted as a function of membrane potential for the currents in C. (E) Whole-cell currents recorded from an outside-out patch during 30-s test depolarizations from −40 to +50 in 10 mV increments. Step potential changes were applied at 3-min intervals. (F) Single channel current recording from a cell-attached patch in the presence of physiological external K^+ (5.4 mM). The patch potential was held −20 mV negative to the cell membrane potential. The patch was repetitively depolarized by 80 mV (assuming a resting potential for the cell of −40 mV, this would correspond to a holding potential of −60 mV and test depolarizations to +40 mV). (G) The averaged current from 33 sweeps is shown below the eight representative current records. The time-course of the averaged current is similar to that recorded from excised patches in which current density was too high to resolve single events (compare with records 2C and 2E) with time constant for inactivation of 939 ms. Current records were filtered at 1 kHz and sampled at 2 kHz. (H) Representative current records from an outside-out patch recording shown at different test potential in the presence of a physiological K^+ gradient. Test potentials are indicated to the right of each sweep. Holding potential was −60 mV. (I) The current/voltage relationship of the unitary currents is given below the current traces. The solid line represents the linear regression to all points and corresponds to a single channel conductance, γ, of 12 pS.

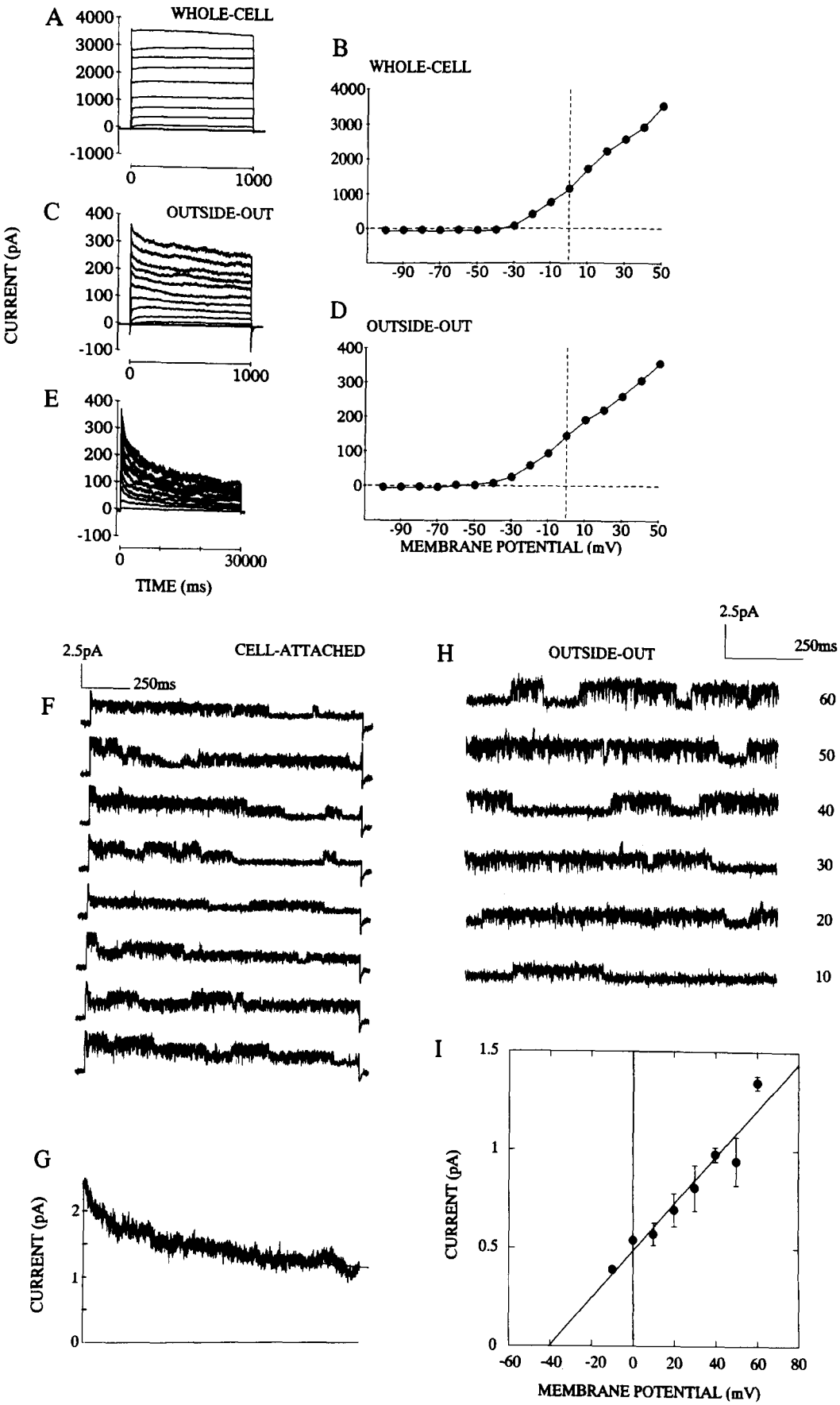
A
WHOLE-CELL
4000
3000
2000
1000
0
-1000
0
1000
B
WHOLE-CELL
4000
3000
2000
1000
0
-90 -70 -50 -30 -10 10 30 50
C
OUTSIDE-OUT
400
300
200
100
0
-100
0
1000
D
OUTSIDE-OUT
400
300
200
100
0
-90 -70 -50 -30 -10 10 30 50
MEMBRANE POTENTIAL (mV)
CURRENT (pA)
E
400
300
200
100
0
-100
0
30000
TIME (ms)
2.5pA
250ms
F
CELL-ATTACHED
G
CURRENT (pA)
2
1
0
H
OUTSIDE-OUT
2.5pA
250ms
60
50
40
30
20
10
I
1.5
1
0.5
0
-60 -40 -20 0 20 40 60 80
MEMBRANE POTENTIAL (mV)
CURRENT (pA)

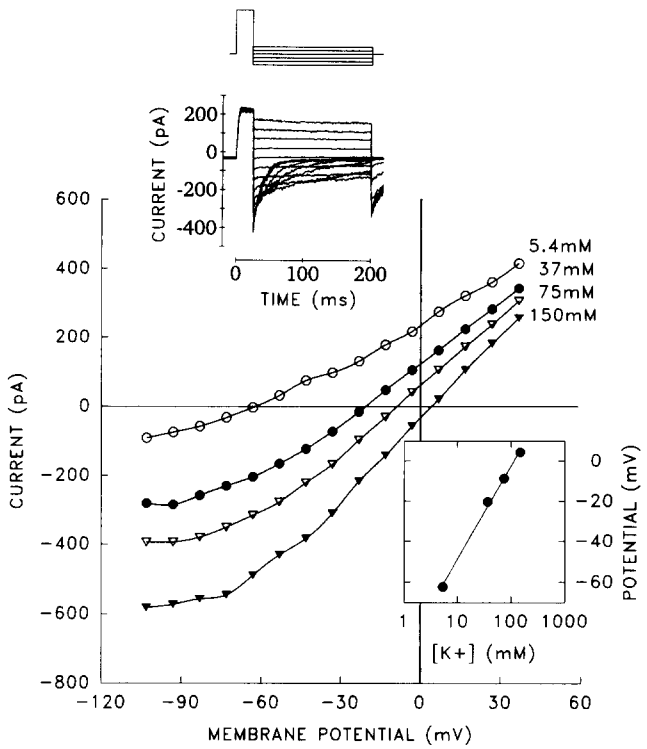

Fig. 3. Selectivity of hPCN1/Kv1.5 currents in excised patches from transfected CHO cells. Current selectivity was determined from shifts in the tail current reversal potential in excised outside-out patches. Current traces are shown in the upper inset. Currents elicited by depolarization to +50 mV followed by repolarization to potentials ranging from +40 mV (upper trace) to −100 mV (lower trace) are shown superimposed. The voltage protocol is shown above the current traces. The external solution in this record contained 150 mM K^+. Peak tail current amplitude is shown as a function of increasing external K^+ concentration (shown to the right of each trace). NaCl in the external solution was isoosmotically replaced with increasing amounts of KCl. Shifts in the current reversal as a function of increasing external K^+ concentration is plotted in the lower inset. The solid line is the best fit to the data points and with a slope of 46.3 per decade change in external K^+ concentration which is to be compared to the predicted Nernstian slope of 59 mV.

obtained from eighteen cells was -33 ± 3.0 mV with a slope of 3.9 ± 0.8 mV. The mean potential for half-maximal current activation determined in eleven cells was -19 ± 3.0 mV with a slope of -6.5 ± 0.9 mV. Maximal conductance levels were reached at potentials greater than +20 mV. Superposition of the two curves, steady-state inactivation and activation, revealed a 'window' of voltage where channels are available for activation without completely inactivating.

The voltage dependence of recovery from inactivation was determined in experiments similar to that depicted in Fig. 4C. The time-course for recovery from inactivation decreased with increasing hyperpolarization. The time constants for recovery at the most hyperpolarized potential of −140 mV were 0.19 ± 0.08 and 0.69 ± 0.21 s ($n = 13$) as compared to values of 3.1 ± 1.8 ($n = 8$) and 55.6 ± 8.9 s ($n = 7$) obtained at −70 mV.

The kinetics of channel closure was determined from fits to tail current data over the voltage range where channel activation was not observed. Time constants for current deactivation as a function of voltage are given in 4D. The voltage dependence of K^+ current kinetics obtained in outside-out patches is summarized in Fig. 4D.

A transfected stable CHO cell line expressing the hPCN1-cp chimera was characterized as above in whole-cell and outside-out patches. No significant differences could be discerned in current kinetics between hPCN1/KV1.5 and hPCN1-cp expressing cells. The levels of current expression for hPCN1-cp were equivalent to that obtained for the wild-type channel. Antibodies directed against the transplanted epitope had no effect on channel function when dialyzed intracellularly via the patch pipette or when applied to inside-out patches during 5–30 min exposure, and had no effect on channel block caused by the class III antiarrhythmic clofilium (1 μM), also in inside-out patches (data not shown).

Total cell membrane fractions prepared from the cell line expressing the hPCN1-cp fusion gene and from the cell line expressing the native channel were analyzed on immunoblots, separately employing both the anti-human c-peptide antibody and the antipeptide antibody (anti-h1-(s1 : s2)). The anti-human c-peptide antibody bound to two prominent bands of approx. 82 and 78 kDa as shown in Fig. 5A. This is reasonably close to the predicted mass of 70.1 kDa. The difference in migration is likely due to some combination of the effect of high degree of hydrophobicity, glycosylation, or other post-translational modifications. Bands of lower mass were also detected in deliberately overloaded lanes and probably represent degradation products as they were of increased prominence in membranes prepared in the absence of proteinase inhibitors. Similar blots prepared from *Xenopus* oocyte membranes injected with hPCN1-cp revealed only a single specific diffuse band of about 67–70 kDa among multiple non-specific bands.

Membranes prepared from cells expressing hPCN1-cp were digested overnight with *N*-glycanase and again analyzed by immunoblot using the anti-human c-peptide antibody. As shown in Fig. 5B, the slower migrating band was undetectable after digestion, while the band of 78 kDa appeared to be increased over the control digestion, demonstrating that the 82 kDa band was converted to the 78 kDa band. This suggests that the hPCN1-cp is incompletely glycosylated, although the presence of a few sugar moieties on the faster migrating band cannot be excluded at this level of resolution. These experiments also do not exclude the possibility that the protein is produced without *N*-

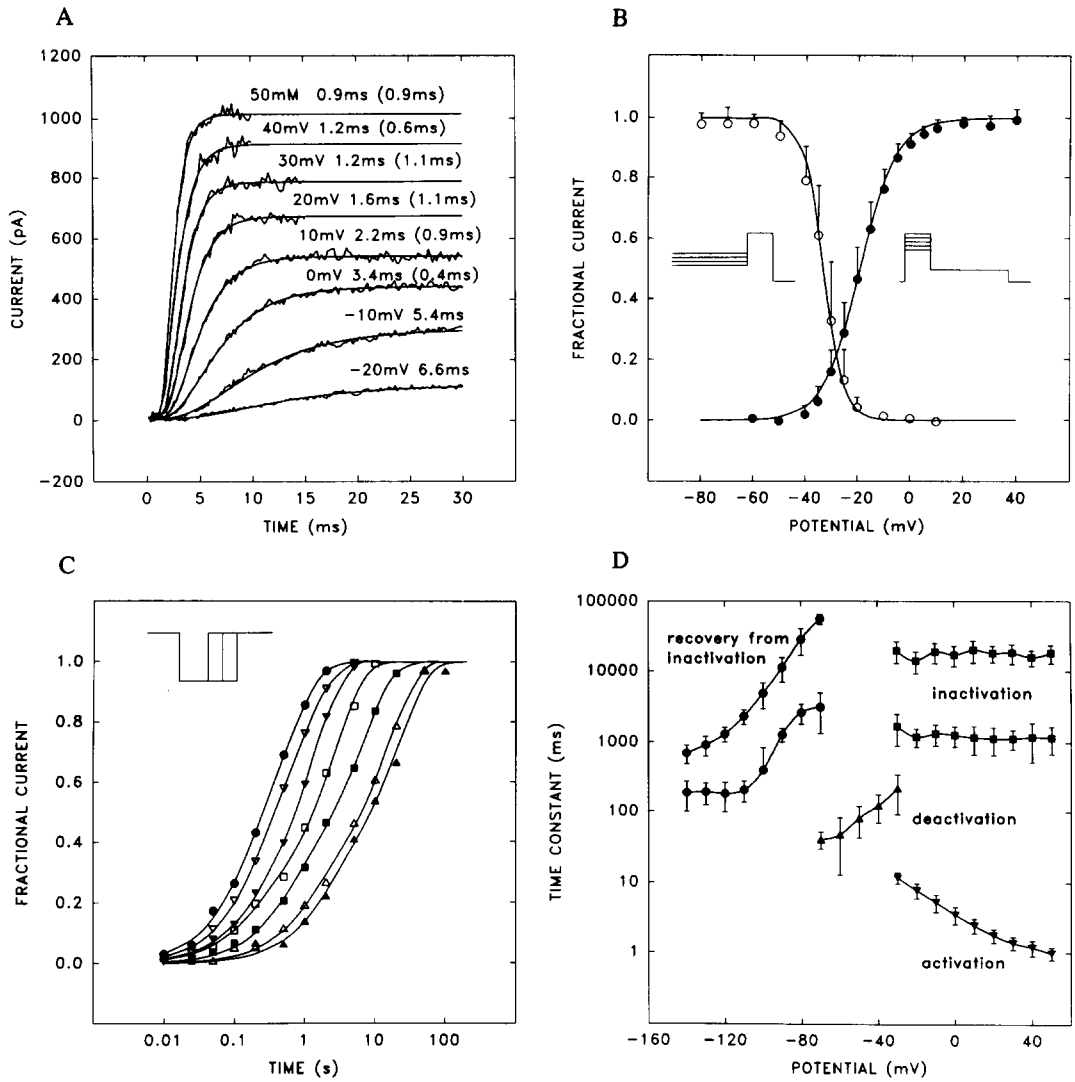

Fig. 4. Voltage dependence of hPCN1/Kv1.5 gating in outside-out patches from transfected CHO cells. (A) Time-course of current activation in a single outside-out patch. The holding potential was −70 mV; depolarizing voltage steps were applied to the voltages indicated above each trace. Current traces were fit according to the relationship given in the text, where A represents the linear leak current component, B represents the peak current amplitude obtained for a given depolarization, and d the delay in current activation. The smooth lines through the data points represent the calculated fits to the activation phase of the outward current records. For depolarizations greater than −10 mV it was necessary to impose a delay d in the current response to the cell to the applied voltage step. The imposed delay is the value in parenthesis above the current trace. The time constant describing current activation at a given voltage is also given above each current trace. (B) Voltage-dependence of inactivation and activation. Steady-state inactivation as well as activation was determined in excised outside-out patches. Activation curves (filled circles) were obtained by measurements of the amplitude of the tail currents at a given time and a fixed potential (−40 mV) following repolarization from various activating potentials. The membrane potential was then stepped to −70 mV for a period of time to allow for full activation at each depolarizing potential. The peak tail current amplitudes were then normalized to the maximal currents obtained at positive activating potentials indicated on the voltage axis according to the relationship: fractional activation = $I_{K,tail}/I_{K,tail,max}$. Data points represent mean values obtained from eleven cells. The smooth line represents the fit through the data points with a Boltzmann distribution of the form $I/I_{max} = \{1+\exp[(V-V_{1/2})/k]\}^{-1}$, where $V_{1/2} = -19$ and $k = -6.5$, mean values determined from fits to the data derived from individual experiments. The parameters of steady-state inactivation (open circles) were determined in experiments in which the holding potential was varied between −80 to +10 mV for 30 s prior to the application of test pulse to +50 mV. Normalized current in response to an activating test pulse of +50 mV is plotted as a function of the conditioning potential indicated on the voltage axis. Data points represent average normalized current values from a total of eighteen cells. The smooth line through the data points represent the average fit to the data with a Boltzmann distribution as above, with $V_{1/2} = -33$ and $k = 3.9$. (C) Time-course of recovery from inactivation. The membrane patch was held at 0 mV for 40 s prior to stepping to various hyperpolarized test potentials to allow for channel recovery for variable periods of time. Curves from left to right correspond to recovery at: −140, −130, −120, −110, −100, −90, −80 mV. The ratio of the current at 0 mV before and after the variable recovery period is plotted as a function of recovery interval. The smooth line represents a double exponential fit to the data points. (D) Summary of the voltage-dependence of K^+ current kinetics obtained from excised outside-out patches. Where multiple time constants were required to obtain an adequate fit to the current data as were in the case for inactivation (measured over a period of 30 s) and recovery from inactivation, both mean time constant values are plotted. Also plotted are deactivation tail current time constants, measured by activating the K^+ conductances with a brief depolarizing pre-pulse then stepping to various potentials in a voltage range hyperpolarized to the current activation threshold. A single exponential was fitted to the decay of tail currents recorded during repolarization.

linked oligosaccharide by glycosidase processing rather than by escaping co-translational glycosylation. Membranes prepared from cells at days 1 through 5 after passage showed an increase in the ratio of the 82 kDa band to the 78 kDa band with increasing time in culture (data not shown). This may be a reflection of the state of confluency, a slower rate of growth, or both, allowing more of the protein to be glycosylated.

The antipeptide antibody, anti-h1-(s1:s2), directed at a sequence in the first extracellular membrane spanning domain (amino acid 281–305), also detected the two bands of 82 and 78 kDa from cells expressing hCN1-cp, and two major bands of approx. 78 and 70 kDa in membranes prepared from cells expressing the native hPCN1/Kv1.5 protein, as shown in Fig. 5C. No significant levels of other bands were detected with either antibody. These results suggest that there was no significant cleavage of the c-peptide addition (or other C-terminal processing) from the rest of the chimeric protein. It is important to note that this is the first direct demonstration of the intact protein in a stable transfected cell line.

Anti-h1-(s1:s2) antibody was employed to determine if cell sorting techniques could be used to obtain cultures highly enriched for positive cells. Cell lines that were originally highly enriched for hPCN1-cp ex-

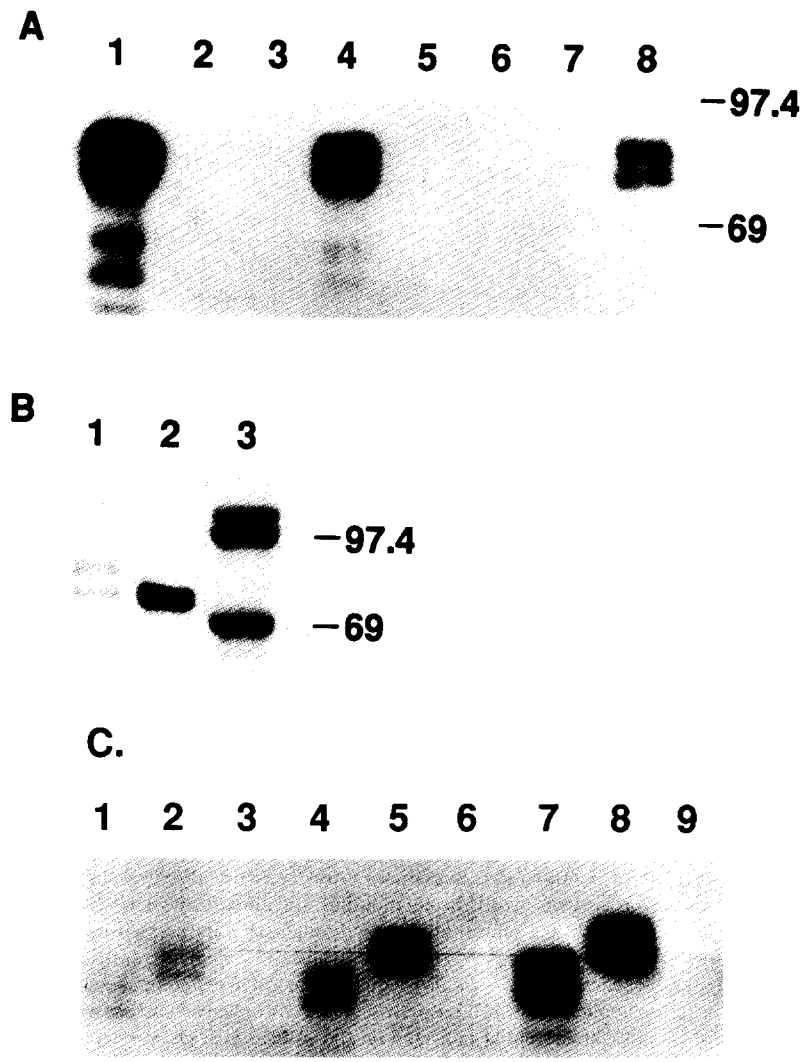

Fig. 5. (A) Immunoblot analysis of hPCN1-cp expressing cells. Cell membranes were analyzed in immunoblots probed with anti-human proinsulin c-peptide antibody. Lanes 1, 4, 8: membranes from hPCN1-cp expressing cells, 100, 11 and 3 μg protein, respectively; Lanes 2, 5 and 7, identical amounts of native hPCN1-expressing cell membrane protein to lanes 1, 4 and 8; Lane 6, 11 μg of membrane protein from transfected but non-expressing cells. (B) Immunoblot analysis of hPCN1-cp expressing cells before and after *N*-glycanase digestion. Lane 1: 11 μg control hPCN1-cp membranes after overnight digestion in *N*-glycanase buffer excluding enzyme (mock digestion); lane 2: identical reaction including *N*-glycanase; lane 3: ^{14}C-labeled protein standards (marker lane exposed for 36 h and added to figure as composite). (C) Immunoblot comparing hPCN1 and hPCN1-cp, employing an antipeptide antibody directed at the first extracellular loop as described in the text. Cell membranes were prepared from cells expressing hPCN1 (Lanes 1, 4, 7), or hPCN1-cp (Lanes 2, 5, 8), and G418-resistant but non-channel expressing controls (Lanes 3, 6, 9). Lanes were loaded with approx. 3 (1–3), 11 (4–6) and 33 (7–9) μg of membrane protein.

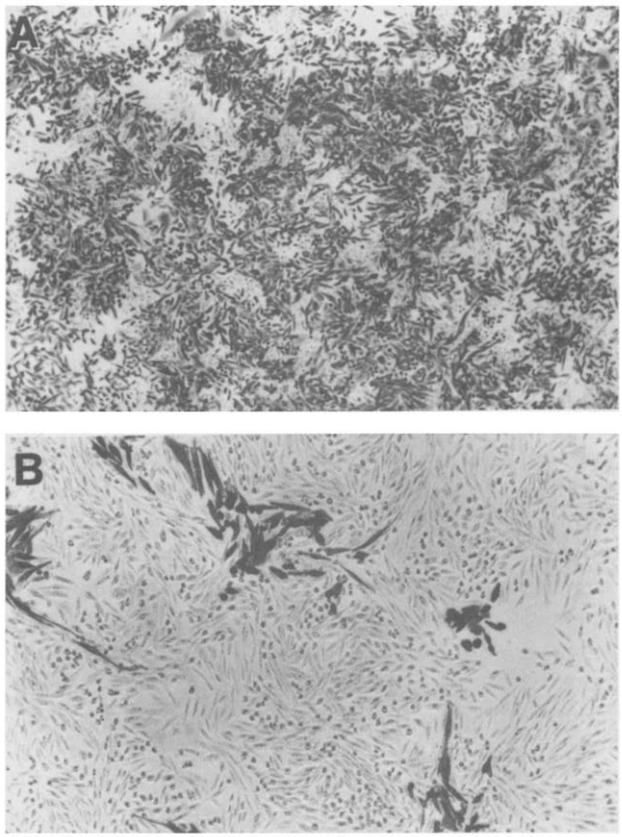

Fig. 6. Immunohistochemical detection of CHO cells expressing hPCN1-cp separated by FACS. Antisera prepared against the peptide H1(s1-s2) LLRHPPAPHQPPAPAP-GANGSGVMA (in the first putative extracellular loop) was employed to sort transfected cells expressing hPCN1-cp. Cells were treated in the following order: rabbit anti-H1(s1-s2) antisera; biotinylated goat anti-rabbit IgG; avidin conjugated with phycoerythrin. Cells were fixed in 3% formaldehyde, permeabilized with 0.1% Triton X-100, and treated consecutively with: rabbit anti-human-c-peptide antisera at various dilutions; goat biotinylated anti-rabbit IgG; (Biotin-HRP)-avidin complex; and finally DAB substrate. Top: cells sorted to be 90+% positive using the antipeptide antibody, then stained with the anti-human c-peptide antibody. Bottom: cells sorted to be less than 10% positive for the surface antigen, and stained as previously described.

pression were found to be overgrown by non-expressing cells in just a few passages. To verify that this was due to overgrowth of cells that did not express the protein as opposed to accumulation of mutations that would merely inactivate channel function, an enriched population was sorted preparatively. The culture which had been originally greater than 90% positive was reduced to 8.17% positive. The positive cells were immediately re-sorted, and confirmed to be 88.7% positive. The sorting data were confirmed by histochemical staining of the separated positives and negatives using the anti-c-peptide antibody, as shown in Fig. 6. After 15 additional passages the percent positive cells had fallen to 45% from 88.7%.

Discussion

Mammalian K^+ channels related to the *Shaker* locus of *Drosophila* share common structural domains which include a C-terminal cytoplasmic region of variable length in which are found putative phosphorylation sites, Ca^{2+} binding sites, or cyclic nucleotide binding sites [1,5,6]. The hPCN1/Kv1.5 delayed rectifier channel has a C-terminal cytoplasmic domain of 98 amino acids, which contains two consensus sequences for cAMP-dependent phosphorylation, three putative casein-kinase II (CK2) phosphorylation sites and two putative protein kinase C phosphorylation sites [10]. The mammalian Kv1.x channels share a common conserved termination sequence with *Drosophila Shaker* channels of threonine-(aspartic or glutamic acid)-(leucine or valine), although the intervening region beginning from 20 amino acids after the last hydrophobic sequence is highly divergent [10,19–22]. While the function of this region is still uncertain, channels with a C-terminal deletion have been shown to act as dominant-negative mutations, interfering with the expression of normal subunits [8].

We have studied the C-terminal domain of the human K^+ channel hPCN1/Kv1.5 in a mammalian cell line by comparing expression of the wild-type channel with a chimeric channel having a short C-terminal extension. Initial results showed that expression levels in both cases were high. Calculated current density for the wild-type channel in outside-out patches at 0 mV was 1500 pA/pF, estimating an average area for an outside-out patch of approx. 10 μm^2 for pipettes of the resistance used in our experiments [23]. Assuming that all channels are open at peak current during a large depolarization, and using the experimentally determined values for single channel current and for average peak current in outside-out patches at 0 mV (0.5 and 150 pA, respectively), the calculated channel density in the transfected CHO cells was 30 per μm^2. Given an average cell capacitance of 30 pF, we estimate 90000 channels per cell making no corrections for inactivation at the holding potential. This density would be increased if the area of the membrane patch were less than 10 μm^2. Expressed in terms of cell capacity, the channel density would be approx. 3000/pF.

Midpoints of steady-state activation and inactivation were shifted by approx. 10 mV in the hyperpolarized direction in excised patches from the transfected CHO cells in comparison to similar data obtained from *Xenopus* oocytes [10]. A comparison of the threshold for current activation in the whole-cell versus the excised patch also revealed a similar hyperpolarizing

shift. This is likely to be due to the dissipation of Donnan-type potentials in the excised patch. These effects are negligible in the case of the oocyte two-microelectrode voltage clamp recordings and time-dependent in the case of whole-cell recordings due to limited dialysis of the cell with the pipette solution. Similar shifts in the voltage-dependent properties have been observed for Na^+ currents in rat clonal pituitary cells (GH_3) when compared in membrane patch and whole-cell recordings (e.g., Ref. 24).

Further characterization of the expression of hPCN1/Kv1.5 in CHO cells showed the presence of multiple inactivation states. At all holding potentials (-70 to -140), two components of recovery were discernible with time-courses which were highly voltage dependent. Current inactivation was well described as a double-exponential process with time constants of 1 and 17 s at 0 mV, respectively. The rate of inactivation was voltage independent over the voltage range of -30 to $+50$ mV.

In contrast to the time-course of inactivation, channel activation was highly voltage dependent and considerably faster than inactivation. Our kinetic data are similar to those observed for RCK1 characterized in Sol-8 cells suggesting a kinetic scheme in which channel activation and inactivation are kinetically coupled and in which inactivation proceeds with little contamination by activation [25].

A chimeric hPCN1-human proinsulin c-peptide construct (hPCN1-cp) was prepared by a PCR-gene fusion technique. Studies of stable CHO cell lines expressing the chimeric channel revealed no significant changes in the kinetic properties of hPCN1-cp as compared to the wild-type channel despite the 32 amino acid extension on the C-terminal, which buried the highly conserved *Shaker*-related T-D/E-L/V terminating sequence. Injection of the anti-c-peptide antibody into cells, or applying the antibody to inside-out patches, expressing the hPCN1-cp gene had no significant effect on channel activation or inactivation, suggesting that the free end of this channel has no major role in these processes.

That the chimeric channel could be visualized by immunohistochemical methods via its transplanted epitope confirmed the amino acid sequence previously deduced from the genomic and cDNA sequences [10]. The human Kv1.5-like sequence of Curran et al. [9] differs from other human and rodent Kv1.5 sequences primarily at the 3′ end, the result of a two base (GG) deletion causing a frame-shift [10,22,26,27]. As more variant isoforms of ion channels are reported, it will be necessary to confirm the predicted protein sequence especially when a single gene is thought to be present [9].

Immunoblots of cells expressing hPCN1-cp probed with the anti-c-peptide antibody or the antipeptide antibody directed at the first extracellular loop revealed two bands, at approx. 82 and 78 kDa, both greater than the predicted mass of 70.1 kDa. Immunoblots of cells expressing the wild-type hPCN1/Kv1.5 channel also showed two bands of similar intensity when probed with the same antipeptide antibody. The similarity of immunoblots probed with an internal or C-terminal antibody suggests that there was no significant cleavage of the peptide chain of the fusion protein. The 82 kDa band was completely converted to the 78 kDa band by digestion with *N*-glycanase, showing that the hPCN1-cp chimera was incompletely *N*-glycosylated. Two mammalian *Shaker*-like isoforms lack a *N*-linked glycosylation site in the first extracellular loop, HK2/Kv1.5 [26] and HSBK2/Kv1.6 [21], and both have been found to be functional in oocyte or mammalian expression systems. This suggests that incompletely *N*-glycosylated hPCN1/Kv1.5 may still be correctly inserted into intracellular membranes and transported to the cell surface. Evidence for post-translational modification of *Shaker*-like mammalian K^+ channels has also been suggested in a report showing that immunoblots of the rodent brain channel Kv1.4 showed a diffuse band of 95 kDa from brain but only 88 kDa after in vitro translation (compared to 71 kDa predicted) [28]. Similar findings, suggesting that high-level expression leads to saturation of the *N*-glycosylation system, have been recently reported for the rat skeletal muscle $\mu 1$ Na^+ channel and the rat *N*-methyl-D-aspartate receptor expressed transiently in human embryonic kidney 293 cells, both of which show a high concentration of non-*N*-glycosylated protein [29,30].

In mixed cultures of transfected cells, some expressing and some not expressing the hPCN1-cp gene, the non-expressing cells overgrew the expressing cells. The slowed growth of cells expressing high levels of K^+ channels relative to controls could be due several possibilities. The decrease in growth rate may be the direct result of diverting significant cellular resources to producing the transfected gene or alternatively to a dampening of the normal oscillatory changes in K^+ permeability which may occur during the cell cycle [29,30]. This observation provides direct experimental evidence for the hypothesis put forward by Koren et al. [25] who suggested that cells expressing a larger number of delayed rectifier K^+ channels might be put at a growth disadvantage.

The high level of channel expression in the stable hPCN1/Kv1.5 and hPCN1-cp expressing CHO cell line constitutes an ideal system for studying K^+ channel post-translational events, regulation, and pharmacology in a mammalian environment. High-level expression systems such as these will prove valuable to examine domain-specific targeting to specific subcellular regions [28], perhaps by gene expression in primary cultures via viral vectors [31].

Acknowledgements

We thank Dr. D.F. Steiner, in whose laboratory some of these experiments were performed, and Drs. R. Miller, H. Fozzard and K.S. Polonsky for critical reading of the manuscript. Funding was provided by The Marilyn M. Simpson Charitable Trust (L.H.P.), NIH Program Project PO1 DK44840 (L.H.P. and D.J.N.), JDFI Research Grant and ADA Research and Development Award (L.H.P.), and RO1 GM36823 and PO1 NS24575 (D.J.N.).

References

1 Kaczmarek, L.K. (1991) New. Biol. 3, 315–23.
2 Perney, T.M. and Kaczmarek, L.K. (1991) Curr. Opin. Cell. Biol. 3, 663–70.
3 Hoshi, T., Zagotta, W.N. and Aldrich, R.W. (1990) Science 250, 533–250.
4 Li, M., Jan, Y.N. and Jan, L.Y. (1992) Science 257, 1225–30.
5 Atkinson, N.S., Robertson, G.A. and Ganetzky, B. (1991) Science 253, 551–555.
6 Guy, H.R., Durell, S.R., Warmke, J., Drysdale, R. and Ganetzky, B. (1991) Science 254, 730.
7 Vandogen, A.M.J., Frech, G.C., Drewe, J.A., Joho, R.H. and Brown, A.M. (1990) Neuron 4, 433–443.
8 Gisselmann, G., Sewing, S., Madsen, B.W., Mallart, A., Angaut-Petit, D., Muller-Holtkamp, F., Ferrus, A. and Pongs, O. (1989) EMBO J. 8, 2359–2364.
9 Curran, M.E., Landes, M.G. and Keating, M.T. (1992) Genomics 12, 729–737.
10 Philipson, L., Hice, R.E., Schaefer, K., LaMendola, J., Bell, G.I., Nelson, D.J. and Steiner, D.F. (1991) Proc. Natl. Acad. Sci. USA 88, 53–57.
11 Krieg, P.A. and Melton, D.A. (1987) Proc. Natl. Acad. Sci. USA 84, 2331–5.
12 Andersson, S., Davis, D.N., Dahlback, H., Jornvall, H. and Russell, D.W. (1989) J. Biol. Chem. 264, 8222–8229.
13 Yon, J. and Fried, M. (1989) Nucleic Acids Res. 17, 4895.
14 Bell, G.I., Pictet, R.L., Rutter, W.J., Cordell, B., Tischer, E. and Goodman, H.M. (1980) Nature 284, 26–32.
15 Saiki, R.K., Scharf, S., Faloona, F., Mullis, K.B., Horn, G.T., Erlich, H.A. and Arnheim, N. (1985) Science 230, 1350–1354.
16 Hamill, O.P., Marty, A., Neher, E. and Sakmann, B. (1981) Pflügers Arch. 391, 85–100.
17 Sambrook, J., Fritsch, E.F. and Maniatis, T. (1989) Molecular Cloning: A Laboratory Manual, 2nd Edn., Cold Spring Harbor Lab., Cold Spring Harbor, NY.
18 Seino, S., Chen, L., Seino, M., Blondel, O., Takeda, J., Johnson, J.H. and Bell, G.I. (1992) Proc. Natl. Acad. Sci. USA 89, 584–588.
19 Tempel, B.L., Jan, Y.N. and Jan, L.Y. (1988) Nature 332, 837–839.
20 Stuhmer, W., Ruppersberg, J.P., Schroter, K.H., Sakmann, A., Stocker, M., Giese, K.P., Perschke, A., Baumann, A. and Pongs, O. (1989) EMBO J. 8, 3235–3244.
21 Grupe, A., Schroter, K.H., Ruppersberg, J.H., Stocker, M., Drewes, T., Beckh, S. and Pongs, O. (1990) EMBO J. 9, 1749–1756.
22 Swanson, R., Marshall, J., Smith, J.S., Williams, J.B., Boyle, M.B., Folander, K., Luneau, C.J., Antanavage, J., Olivia, C., Buhrow, S.A., Bennet, C., Stein, R.B. and Kaczmarek, L.K. (1990) Neuron 4, 929–939.
23 Sakmann, B. and Neher, E. (1983) Geometric parameters of pipettes and membrane patches, in Single-Channel Recording (Sakmann, B. and Neher, E., eds.), pp. 37–52, Plenum Press, New York.
24 Fernandez, J.M., Fox, A.P. and Krasne, S. (1984) J. Physiol. 356, 565–585.
25 Koren, G., Liman, E.R., Logothetis, D.E., Nadal-Ginard, B. and Hess, P. (1990) Neuron 2, 39–51.
26 Tamkun, M.M., Knoth, K.M., Walbridge, J.A., Kroemer, H., Roden, D.M. and Glover, D.M. (1991) FASEB J. 5, 331–337.
27 Roberds, S.L. and Tamkun, M.M. (1991) Proc. Natl. Acad. Sci. USA 88, 1798–1802.
28 Sheng, M., Tsaur, M.L., Jan, Y.N. and Jan, L.Y. (1992) Neuron 9, 271–84.
29 Ukomadu, C., Zhou, J., Sigworth, F.J. and Agnew, W.S. (1992) Neuron 8, 663–76.
30 Chazot, P.L., Cik, M. and Stephenson, F.A. (1992) J. Neurochem. 59, 1176–1178.
31 Karschin, A., Thorne, B.A., Thomas, G. and Lester, H.A. (1992) Methods Enzymol 207, 408–23.